Phosphotransfer and CheY-Binding Domains of the Histidine Autokinase CheA Are Joined by a Flexible Linker†

Hongjun Zhou,‡ Megan M. McEvoy,‡ David F. Lowry,‡ Ronald V. Swanson,§,|| Melvin I. Simon,§ and Frederick W. Dahlquist*,‡

Institute of Molecular Biology, University of Oregon, Eugene, Oregon 97403, and Department of Biology, California Institute of Technology, Pasadena, California 91125

Received August 19, 1995; Revised Manuscript Received November 13, 1995⊗

ABSTRACT: Multidimensional heteronuclear NMR techniques were applied to study a protein fragment of the histidine autokinase CheA from *Escherichia coli*. This fragment ($CheA_{1-233}$) contains the phosphotransfer domain and the CheY-binding domain joined by a linker region. Comparison of chemical shift and NOE cross-peak patterns indicates that the structures of the two domains in $CheA_{1-233}$ remain nearly the same as in the two individual domain fragments, $CheA_{1-134}$ and $CheA_{124-257}$. Relaxation properties of the backbone ^{15}N nuclei were measured to study the rotational correlations of the two domains and properties of the linker region. Dynamics data were analyzed both by an isotropic motional model and an anisotropic motional model. The experimental T_1 and T_2 values, the derived rotational correlation times, and motional anisotropy are significantly different for the two domains, indicating the two domains reorient independently and the linker region is highly flexible. Dynamics data of $CheA_{1-233}$ were also compared with those of $CheA_{1-134}$. Our studies show that flexible domain linkers and extended and flexible terminal polypeptide chains can have significant effects on the motional properties of the adjacent structured regions. These observations suggest a model for the graded regulation of CheA autophosphorylation activity. In this model, the various activity states of the receptor are generated by controlling the access of the mean position of the kinase domain to the phosphotransfer domain. This would then modulate the diffusional encounter rate of the domains and hence activity over a wide and graded range of values.

The histidine autokinase CheA from *Escherichia coli* is a central component of the chemotaxis system which controls the cell response to chemical stimuli. In the signal transduction cascade the periplasmic domains of the membrane-spanning receptors sense changes in the ligand-binding states and transmit the signal to their cytoplasmic domains. The autophosphorylation rate of CheA is regulated through ternary protein complexes formed by the cytoplasmic domains of the receptors, the coupling protein CheW, and the protein kinase CheA (Gegner et al., 1992; Milburn et al., 1991; Borkovich et al., 1989; Borkovich & Simon, 1990; Ninfa et al., 1991). Phosphorylated CheA donates its phosphoryl group to the response regulator protein CheY (Hess et al., 1988a; Stock et al., 1988; Sanders et al., 1989) or CheB (Lupas & Stock, 1989; Ninfa et al., 1991), which are sequestered by the substrate binding domain of CheA (Swanson et al., 1993; Morrison & Parkinson, 1994). Phospho-CheY controls the direction of flagellar rotation, and phospho-CheB regulates the receptor adaptation (Stewart & Dahlquist, 1987; Bourret et al., 1991; Roman et al., 1992; Stock et al., 1989; Borkovich et al., 1992).

Full-length CheA from *E. coli* has 654 residues and was shown to consist of separable functional domains joined by linker regions (Figure 1) (Swanson et al., 1993; Parkinson & Kofoid, 1992; Morrison & Parkinson, 1994). Its kinase domain resides in the central region. Its amino-terminal 134 residues form the phosphotransfer domain which contains the site of autophosphorylation, His48 (Hess et al., 1988b; Swanson et al., 1993; Morrison & Parkinson, 1994). The CheY-binding domain is formed by residues 159−227 (Morrison & Parkinson, 1994; Swanson et al., 1993; McEvoy et al., 1995). Isolated domain fragments retain their functions (Swanson et al., 1993; Morrison & Parkinson, 1994). The linker regions of CheA include one or several prolines and a preponderance of charged and polar residues. These regions were shown to be more susceptible to proteolytic attack than other parts of the molecule (Morrison & Parkinson, 1994). The functional roles of the linker regions in the signal transduction pathway have not been fully understood.

High-resolution NMR[1] techniques have been applied to study the structure, function, and dynamics of the phospho-

† D.F.L. was supported by a Cancer Research Fund of the Damon Runyon-Walter Winchell Foundation Fellowship DRG-1195. M.M.M. is supported by an NIH training grant. R.V.S. was supported by a National Research Service Award Fellowship GM14767 from NIH. This work was supported by research grants GM33677 (F.W.D.) and AI-19296 (M.I.S.).

* Author to whom correspondence should be addressed.

‡ University of Oregon.

§ California Institute of Technology.

|| Present address: Department of Molecular Biology, Industrial BioCatalysis Inc., 512 Elmwood Ave., Sharon Hill, PA 19079.

⊗ Abstract published in *Advance ACS Abstracts,* December 15, 1995.

[1] Abbreviations: HSMQC, heteronuclear single-multiple-quantum coherence; NOE, nuclear Overhauser effect; NOESY, nuclear Overhauser effect spectroscopy; TOCSY, total correlation spectroscopy; HMQC, heteronuclear multiple-quantum coherence; HSQC, heteronuclear single-quantum coherence; 2D, two dimensional; 3D, three dimensional; NMR, nuclear magnetic resonance.

0006-2960/96/0435-433$12.00/0

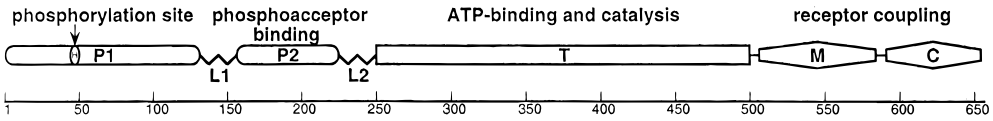

FIGURE 1: Schematic representation of the constituent functional domains of CheA [see McEvoy et al. (1995)].

transfer domain (P1) (Zhou et al., 1995) and the CheY-binding domain (P2) (McEvoy et al., 1995) in aqueous solution. The P2 fragment used in the study, $CheA_{124-257}$, includes the linker region (residues 135−158) joining the P1 and P2 domains of CheA and a small sequence that is helical in the phosphotransfer domain, $CheA_{1-134}$. These regions were found to be highly flexible in $CheA_{124-157}$. Another protein fragment, $CheA_{1-233}$, which sequentially encodes the phosphotransfer, the linker, and the CheY-binding regions, was shown to retain its functional activities (Swanson et al., 1993). In order to reveal possible structural changes of the two domains in $CheA_{1-233}$ from the isolated domain fragments, interdomain interaction, and properties of the linker region, we have studied $CheA_{1-233}$ using heteronuclear multidimensional NMR techniques.

MATERIALS AND METHODS

Sample Preparation. To express histidine-tagged and ^{15}N-uniformly labeled $CheA_{1-233}$, strain M15/pREP4/pRS1−4 (Swanson et al., 1993) was grown at 37 °C in M9 minimal medium with $^{15}NH_4Cl$ (1 g/L) as the sole nitrogen source. Expression and purification procedures are essentially the same as described by Swanson et al. (1993).

Protein samples were dialyzed against 50 mM $NaPO_4$, pH 8.0, and concentrated to approximately 2 mM. One sample was subsequently transferred into 50 mM $NaPO_4$, pH 6.3, buffer. 5% D_2O and 0.02% sodium azide were added to the final NMR samples.

NMR Data Collection and Processing. All data reported in this paper were collected on a General Electric Omega 500 MHz spectrometer at pH 6.3, 30 °C except as otherwise stated. Data collection and processing were essentially the same as described by Zhou et al. (1995). 2D $^1H-^{15}N$ HSMQC (Zuiderweg, 1990) and 3D ^{15}N-edited NOESY (Kay et al., 1989b; Zuiderweg et al., 1989) and TOCSY (Cavanagh et al., 1989; Marion et al., 1989) were recorded as described for $CheA_{1-134}$ (Zhou et al., 1995). For the 3D ^{15}N-edited NOESY, the mixing time was set to 120 or 90 ms. For the 3D ^{15}N-edited TOCSY, the mixing time was set to 60 ms. A series of HSQC-J spectra (Billeter et al., 1992) with eight time delays, 15, 30, 50, 70, 80, 90, 115, and 130 ms, was collected to measure the $^3J_{HN\alpha}$ coupling constants. The T_1, T_2 values of ^{15}N nuclei, and the $^{15}N\{^1H\}$ NOE values were measured using inverse detected two-dimensional NMR spectroscopy (Kay et al., 1989a; Clore et al., 1990; Barbato et al., 1992). To obtain T_1 relaxation rates, seven delays of 28, 70, 140, 308, 505, 645, and 841 ms were employed. To obtain T_2 relaxation rates, seven delays of 7.6, 23, 46, 69, 99, 122, and 161 ms were employed. $^3J_{HN\alpha}$ values, T_1, T_2 of ^{15}N nuclei, and $^{15}N\{^1H\}$ NOE were extracted as described by Zhou et al. (1995). Uncertainties in measured peak heights were estimated from baseline noise level (σ_{noise}). The actual values used in the fitting of T_1 and T_2 were slightly higher than σ_{noise} to take into account other possible errors. Typical values for σ_{noise} were less than 5% of the peak heights in the first T_1 or T_2 data sets. A constant error of ±0.05 was given to all measured NOE factors. This error range was estimated from two sets of experiments for NOE measurement.

Backbone Dynamics. Relaxation data were analyzed using both an isotropic model and an anisotropic model introduced by Lipari and Szabo (1982). Equations and parameters relating T_1, T_2, and NOE factor of an amide ^{15}N spin are the same as eqs 1−3 of Kay et al. (1989a). For isotropic motions with overall rotational correlation time τ_m and effective correlation time τ_e of rapid internal motions, the spectral density function is given by (Lipari & Szabo, 1982)

$$J(\omega) = S^2\tau_m/[1 + (\omega\tau_m)^2] + (1 - S^2)\tau/[1 + (\omega\tau)^2] \quad (1)$$

where $1/\tau = 1/\tau_m + 1/\tau_e$, and S^2 is the generalized order parameter, which describes the amplitude of the internal motions. In the anisotropic model, the spectral density is given by (Lipari & Szabo, 1982)

$$J(\omega) = A\{S^2\tau_1/[1 + (\omega\tau_1)^2] + (1 - S^2)\tau_{1e}/[1 + (\omega\tau_{1e})^2]\} + (1 - A)\{S^2\tau_2/[1 + (\omega\tau_2)^2] + (1 - S^2)\tau_{2e}/[1 + (\omega\tau_{2e})^2]\} \quad (2)$$

where $1/\tau_{1e} = 1/\tau_1 + 1/\tau_e$ and $1/\tau_{2e} = 1/\tau_2 + 1/\tau_e$. For a particular amide the mixing parameter A represents the weights of the two modes of rotations represented by the two correlation times τ_1 and τ_2. When internal motions are much faster than overall motions, the above spectral density applies to both axially symmetric and general anisotropic motions (Lipari & Szabo, 1982; Tjandra et al., 1995).

In the present study, we derived the dynamics parameters for each domain by minimizing the function given by (Barbato et al., 1992)

$$f(\tau_m,S^2,\tau_e) = [(T_{1,calc} - T_{1,meas})/\sigma_{T1}]^2 + [(T_{2,calc} - T_{2,meas})/\sigma_{T_2}]^2 + [(NOE_{meas} - NOE_{calc})/\sigma_{NOE}]^2 \quad (3)$$

for each residue, or

$$f(\tau_m,S^2,\tau_e) = \sum_i[(T_{1,calc} - T_{1,meas})/\sigma_{T_1}]^2 + \sum_i[(T_{2,calc} - T_{2,meas})/\sigma_{T_2}]^2 + \sum_i[(NOE_{meas} - NOE_{calc})/\sigma_{NOE}]^2 \quad (4)$$

where the sum extends to all residues in each domain for which the minimization was carried out. These include residues 13−126 for the P1 domain and the residues in the well-defined β strand and α-helical regions for the P2 domain, excluding residues with significant internal motions or high hydrogen exchange rates.

For the isotropic model, the effective correlation time for overall motion was derived by minimizing function 3 or 4 without the last terms contributed by the NOE data. This is a good approximation when internal motions are much faster than overall motions. The S^2 and τ_e values were derived by

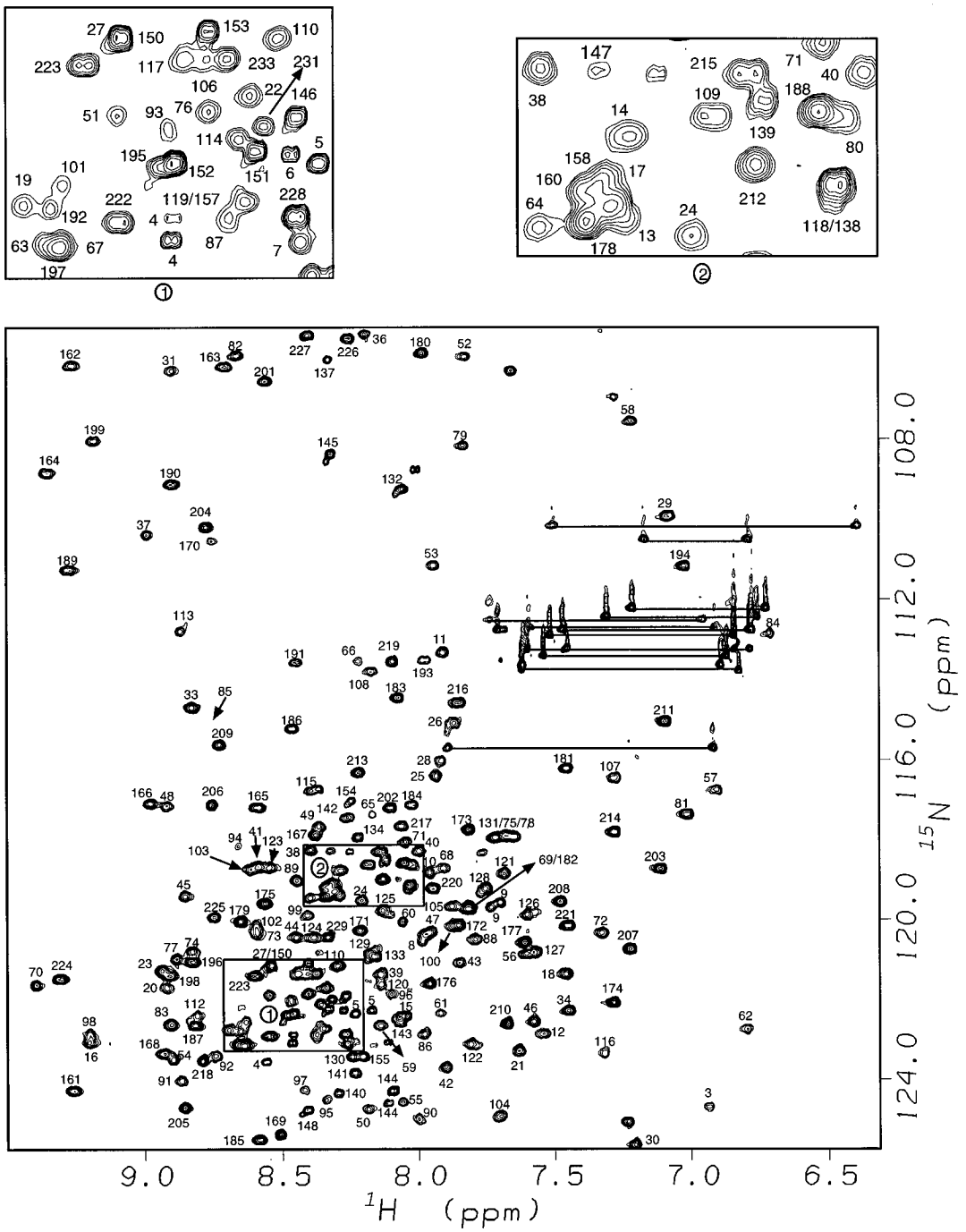

FIGURE 2: ^{1}H−^{15}N HSMQC spectrum of ca. 2 mM uniformly ^{15}N-labeled CheA$_{1-233}$ in 95% H_2O/5% D_2O, 50 mM $NaPO_4$, and 0.02% sodium azide, at 30 °C and pH 6.3. The assignments of the backbone amides are labeled with residue numbers. Side chain NH_2 groups from Asn and Gln residues are shown by straight lines. Expanded regions shown at higher contour level.

minimizing function 3 with the correlation time τ_m set at the best fit values above. For the anisotropic model, τ_e's were set to the values derived from the isotropic model when $\tau_e > 10$ ps and set to 10 ps when $\tau_e < 10$ ps. A global fit was used to find the best global parameters τ_1 and τ_2 by varying them in a 0.2 ns stepsize to minimize function 4. The local parameters S^2 and A were derived for each residue using the best fit τ_1 and τ_2. Errors in the τ_1 and τ_2 fits were estimated from Monte-Carlo simulation and subsequent fitting of the synthesized T_1, T_2, and NOE data (Press et al., 1992; Tjandra et al., 1995). In this procedure random noise with Gaussian distributions and standard deviations of σ_{T1} and σ_{T2} for T_1 and T_2 data, and random noise with uniform distribution within a range of ±0.05 for NOE data were added to 25% of the T_1, T_2, and NOE data points chosen randomly.

RESULTS

Resonance Assignments and Structure Comparison with CheA$_{1-134}$ and CheA$_{124-257}$. Figure 2 shows a ^{1}H−^{15}N correlation spectrum of CheA$_{1-233}$ labeled with the assignments of the backbone amides. At the beginning of this work, NMR assignments and structural studies of the two smaller protein fragments CheA$_{1-134}$ (Zhou et al., 1995) and CheA$_{124-257}$ (McEvoy et al., 1995) were underway. It was realized that the ^{1}H−^{15}N correlation spectrum from CheA$_{1-233}$ is almost a direct overlay of the spectra respectively from CheA$_{1-134}$ and CheA$_{124-257}$ taken under similar conditions.

FIGURE 3: Primary sequence, $^3J_{HN\alpha}$ values, and secondary structure of $CheA_{1-233}$.

This property makes possible a direct transfer of the assignments of the two small protein fragments to $CheA_{1-233}$. For accurate transfer of the assignments, 3D ^{15}N-edited TOCSY and NOESY were taken for $CheA_{1-233}$ and compared with data from $CheA_{1-134}$ and $CheA_{124-257}$. The comparison shows that the chemical shifts of the residues in the two domains of $CheA_{1-233}$ are not significantly different from those in the two small domain fragments. Large but limited chemical shift changes were only observed for a few residues in the C-terminal region of $CheA_{1-134}$ and several residues in the linker region (Figure 4). Therefore, most of the resonances were easily assigned by a direct comparison of the TOCSY and NOESY cross-peak patterns of $CheA_{1-233}$ with those of $CheA_{1-134}$ or $CheA_{124-257}$. The unassigned peaks in the $^1H-^{15}N$ correlation spectrum at this stage belong to those residues with relatively large chemical shift changes from their positions in the individual domains. These peaks were assigned by conventional assignment strategies which consist of a spin system identification step based on the 3D ^{15}N-edited TOCSY and a sequential connectivity identification step based on the 3D ^{15}N-edited NOESY (Wüthrich, 1986; Englander & Wand, 1987). Overall consistency of the assignments was examined and confirmed.

The amide cross-peaks from the linker region can be fairly easily distinguished from those in the structured domains. The linker region gives strong amide proton−side chain proton cross-peaks in the 3D ^{15}N-edited TOCSY but weak or no cross-peaks in the 3D ^{15}N-edited NOESY, suggesting this region is flexible. Three serines, three valines, two alanines, and one threonine in the linker region were identified from the TOCSY. However, sequence-specific assignments of this region based solely on 3D ^{15}N-edited TOCSY and NOESY were difficult. The linker region of approximately 25 residues not only has few residue type variations in the sequence but also is highly flexible, resulting in small ^1H chemical shift dispersion. Additionally, the lack of sequential NOE correlations makes the sequence-specific assignments based on the NOESY spectrum difficult. Nevertheless, these residues have been assigned for $CheA_{124-257}$ through COSY type of experiments using an $^{13}C/^{15}N$-labeled sample (McEvoy et al., 1995). Since the linker region is essentially random coiled in both $CheA_{124-257}$ and $CheA_{1-233}$, the amide and side chain proton chemical shifts are primarily determined by residue type and local sequence. Consequently, the chemical shifts of the residues in this region are nearly the same in the two proteins. This similarity helps in identifying potential crosspeaks to assign to the linker region of $CheA_{1-233}$.

In summary, except for residues M1−M3, S136, S154, S156, I232, the prolines, and the C-terminal histidine tail, all the residues in $CheA_{1-233}$ have been assigned in the $^1H-^{15}N$ spectrum. The assignments of the linker residues agree with results from $CheA_{124-257}$ (McEvoy et al., 1995) and were confirmed by a number of weak NOEs observed for this region in the 3D ^{15}N-edited NOESY. Most of these internal or sequential NOEs are between side chain protons and amide protons and are in the region S136−E148. The region Q150−S158 contains either charged or polar residues in which NOEs were only observed for E152. The pattern of the NOE correlations in the linker region does not characterize any regular secondary structure, indicating this region is flexible but its motion are also restricted by the motions of the two domains.

The small chemical shift differences observed for the P1 and P2 domains in the three protein fragments (excluding residues 124−134 and 234−257 in $CheA_{124-257}$) indicate that there are no stable interdomain contacts. Analysis of the NOESY data suggests that the secondary and tertiary structures of the two domains in $CheA_{1-233}$ are essentially the same as in $CheA_{1-134}$ or $CheA_{124-257}$ (Figure 3). The observed relatively large ^1H and ^{15}N chemical shift differences between $CheA_{1-134}$ and $CheA_{1-233}$ in helices D and E of the phosphotransfer domain indicate subtle structural changes in this region (Figure 4).

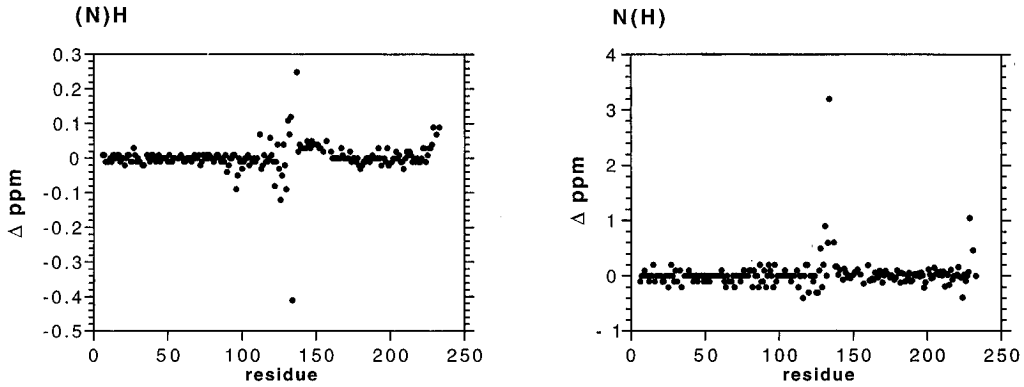

FIGURE 4: Chemical shift differences of the amide ^1H and ^{15}N of $CheA_{1-134}$ (Zhou et al., 1995) and $CheA_{124-257}$ (McEvoy et al., 1995) from those of $CheA_{1-233}$. Residues 124−134 and 234−257 of $CheA_{124-257}$ were excluded from the comparison. The chemical shifts are compared under the following buffer conditions: 95% H_2O/5% D_2O, 50 mM $NaPO_4$, and 0.02% sodium azide, at 30 °C and pH 6.3 (for $CheA_{1-233}$ and $CheA_{1-134}$) or pH 6.5 (for $CheA_{124-257}$). Small reference offsets were adjusted. (Left) Amide proton chemical shift differences. (Right) Amide nitrogen chemical shift differences.

$^3J_{HN\alpha}$ Measurements. The $C^\alpha H$ proton to NH proton coupling constant ($^3J_{HN\alpha}$) is related to the intervening backbone dihetral angle ϕ according to the Karplus equation (Karplus, 1959). Small $^3J_{HN\alpha}$ values (<6 Hz) indicate helical structure and large $^3J_{HN\alpha}$ values (>8 Hz) indicate extended structure (Wüthrich, 1986). The measured $^3J_{HN\alpha}$ values of the two domains of $CheA_{1-233}$ (Figure 3) agree with results from $CheA_{1-134}$ (Zhou et al., 1995) and $CheA_{124-257}$ (McEvoy et al., 1995), indicating similar secondary structures. The $^3J_{HN\alpha}$ values of most residues in the linker region fall in between 6.5 and 7.5 Hz, consistent with a flexible, essentially random coiled, conformation.

Backbone Dynamics. In order to characterize the motional properties of the two domains and the linker region, we measured T_1, T_2, and NOE factors of the backbone ^{15}N nuclei of $CheA_{1-233}$ (Figure 5). A total of 159 T_1 and T_2 values for ^{15}N spins (91 from P1, 13 from the linker, and 55 from P2) have been extracted from the well-resolved peaks.

Isotropic Model. The dynamics data were first analyzed using the isotropic model (eq 1) separately for each residue in the two domains. For residues 10−129 in $CheA_{1-233}$, we have $\langle T_1\rangle = 767 \pm 61$ ms, $\langle T_2\rangle = 75.7 \pm 8.9$ ms, $\langle \text{NOE}\rangle = 0.75 \pm 0.09$, $\langle S^2\rangle = 0.86 \pm 0.07$, and $\langle \tau_m\rangle = 11.7 \pm 0.84$ ns. For residues 160−226 in $CheA_{1-233}$, we have $\langle T_1\rangle = 557 \pm 38$ ms, $\langle T_2\rangle = 106 \pm 16$ ms, $\langle \text{NOE}\rangle = 0.68 \pm 0.08$, $\langle S^2\rangle = 0.86 \pm 0.06$, and $\langle \tau_m\rangle = 7.9 \pm 0.86$ ns. Only residues in the structurally well defined regions were included in the calculation of above average values. Rotational correlation times of 11.7 and 7.9 ns were used for the P1 and P2 domains, respectively, in the calculation of S^2 and τ_e values. Global fit of the dynamics data using eq 4 for selected residues in each domain yields similar effective overall correlations within ±0.2 ns with the average values calculated above.

As shown in Figure 5, the experimental T_1 and T_2 and the theoretically derived effective τ_m values of the two domains are significantly different. The different parameters of the two domains are bridged by those of the linker, which match the values of the adjacent ends of the structured domains and exhibit sharp peaks near the middle (except for T_1 data), as expected for a highly flexible domain linker. The high mobility of the linker is also shown by the negative ^{15}N-$\{^1H\}$ NOE values for the residues in this region (Figure 6).

The $\langle \tau_m\rangle$ value for the helical regions of the P2 domain in $CheA_{1-233}$ is 8.6 ± 0.7 ns, significantly larger than 7.4 ± 0.4 ns for the β sheet region, indicating significant rotational anisotropy. The order parameters of these regions are 0.90 ± 0.04 and 0.84 ± 0.04, respectively. These differences were also observed in $CheA_{124-257}$ (M. M. McEvoy, D. R. Muhandiram, L. E. Kay, and F. W. Dahlquist, manuscript submitted) though with a slightly smaller degree of motional anisotropy. The residues in the P1 domain, however, show much more uniform dynamics parameters.

Anisotropic Model. The analysis of the dynamics data using a simple isotropic model shows that the two domains reorient independently with different degrees and patterns of rotational anisotropy. To confirm the results from this approach and to investigate possible rotational correlations of the two domains, we have further analyzed the dynamics data using an anisotropic model (eq 2). In this model, more parameters are introduced, and the dynamics data cannot be fit individually for each residue. Global fits of τ_1 and τ_2 with τ_e fixed at proper values are made. To locally or globally assign correlation time of internal motions for each residue, results from the isotropic model have been referenced. In the isotropic model, for the P1 domain, fast internal motions were observed for nearly all residues except for the short terminal regions; for the P2 domain, fast internal motions were observed for regions with well defined secondary structures. Our analysis has shown that the derived τ_1 and τ_2 values are stable within a ±0.3 ns range and are insensitive to the exact τ_e values assigned locally for each residue using values from the isotropic model or globally for all residues using a constant value as long as these values are very small (<100 ps). However, the total minimized function values at various τ_1 and τ_2 values were smaller by a factor of 2−3 when τ_e values from the isotropic model were used. In order to make a careful comparison with results from the isotropic model, we have set τ_e values for the anisotropic model to those derived from the isotropic model when these values are above 10 ps and were set to 10 ps for all smaller values. The low τ_e cutoff was used to account for the low sensitivity of the minimization function to τ_e when τ_e is very small.

Using the anisotropic model, we obtained $\tau_1 = 10.6 \pm 0.3$ ns and $\tau_2 = 13.7 \pm 0.4$ ns for the P1 domain and $\tau_1 = 7.0 \pm 0.3$ ns and $\tau_2 = 10.0 \pm 0.3$ ns for the P2 domain. The derived S^2 values for the P1 and P2 domains are only slightly

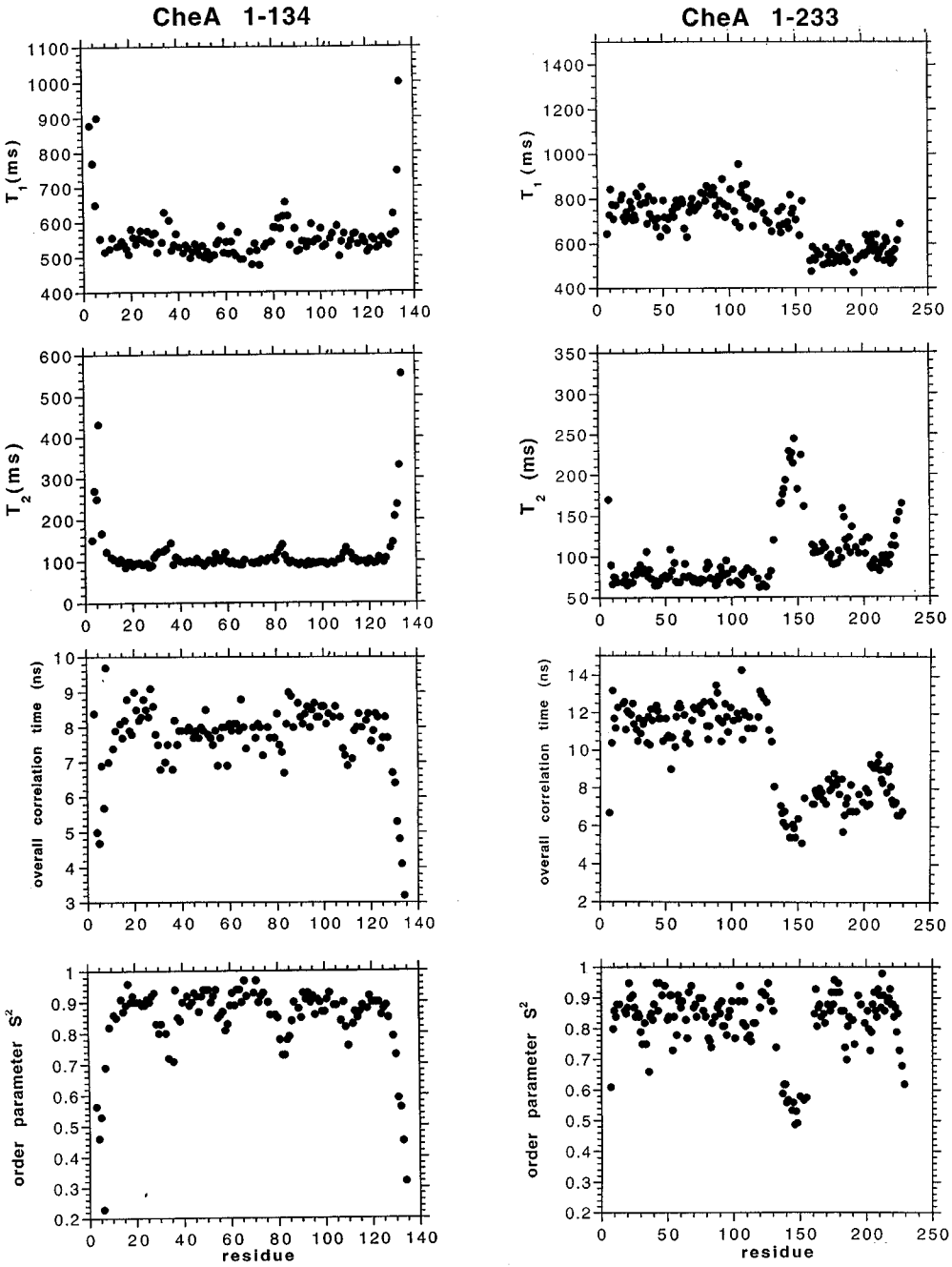

FIGURE 5: Plots as a function of residue number of the measured T_1 and T_2 values, the rotational correlation time τ_m derived from T_1/T_2 ratios, and the order parameter, S^2. (Left panels) $CheA_{1-134}$ (Zhou et al., 1995). (Right panels) $CheA_{1-233}$. The τ_m and S^2 values were derived using a spectral density for the isotropic model. The measured NOE factors, extracted τ_e values, and dynamics parameters for the anisotropic model are included in the Supporting Information.

different from those for the isotropic model for most residues (Table S2, Supporting Information). The motional anisotropy of the P1 domain is small, reflected by the small differences (~25%) in τ_1 and τ_2 values. Residues in the helical regions exhibit a higher degree of slow-mode overall motions. A larger fraction of fast-mode overall motions were found in the turn regions. This difference may result from the differences in the directions of amide bond vectors in the turn regions and the helical regions as compared to the motional axes. The P2 domain has a higher degree of motional anisotropy (~35%). It seems that there is a stronger correlation of the mixing parameters with regions of the structure for the P2 domain (Table S2, Supporting Information). The residues in the sheet region show a larger fraction of fast-mode overall motions while the residues in the helical regions, especially the second helix, show a larger fraction of slow overall motions.

From the anisotropic model, it is again clear that the P1 and P2 domains reorient independently in solution. Different rotational correlation times and properties of rotational anisotropy were observed for the two domains, which are possible only if the linker region is highly flexible and the two domains do not have stable contact. These results suggest that an isotropic model is a good approximation for the P1 domain while motional anisotropy must be considered for the P2 domain.

DISCUSSION

We have used both an isotropic model and an anisotropic model to analyze the dynamics data of $CheA_{1-233}$. Data

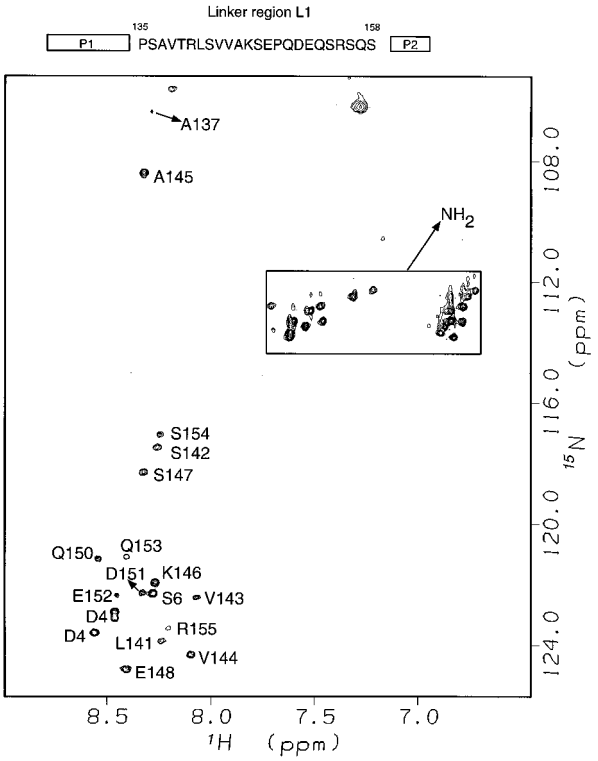

FIGURE 6: Negative contours of the spectrum with $^{15}N\{^1H\}$ NOE effect. The majority of these peaks are from the linker region, S136−S158.

analysis using both models shows unambiguously that the two functional domains in CheA$_{1-233}$ reorient effectively independently and the linker region is highly flexible. This conclusion is supported by the similar chemical shifts between CheA$_{1-233}$ and the two isolated domain fragments. The possibility of stable contacts between the two domains on a time scale much longer than the overall correlation times (∼10 ns) is excluded since such contacts would effectively correlate the motions of the domains.

To evaluate our results in a quantitative manner, we must consider several uncertainties in using different models for the data analysis. An anisotropic model generally introduces more parameters than the experimental observables T_1, T_2, and NOE can possibly uniquely determine for each residue. Global fitting of the two correlation times τ_1 and τ_2 has been used. This approach may make the results sensitive to the selection of the data sets included in the fit and also may make a few "bad" data points dominate the fit while the "good" data points become relatively irrelevant. Therefore, in the anisotropic fit we have only included data from well resolved cross-peaks and residues that do not show internal motions with $\tau_e > 120$ ps calculated from the isotropic fit of the CheA$_{1-134}$ data. Residues with slow internal motions in CheA$_{1-134}$ are mostly in the terminal or flexible turn regions. By excluding these residues, we also have reduced possible errors that may occur because of relaxation or exchange of these amide protons with water. However, to reveal the motional anisotropy of a molecule, it is necessary to include in the fit as many residues as possible with different orientations of amide bond vectors with respect to the motional axes. This was achieved by including residues both in the helical regions and some residues in the turn regions for the P1 domain and residues both in the β-sheet region and the helical regions for the P2 domain. Because of the high hydrogen exchange rates, the T_1 and T_2 values and the derived dynamics parameters of the linker region should only be considered qualitively.

In CheA$_{1-233}$ we observe that the differences in the extracted S^2 values from the isotropic model and the anisotropic model are small (<5%) for most residues. The correlations of the order parameters with the secondary structure and local structural flexibilities are clear. In the P1 domain, the turn regions and the terminal regions clearly show lower order parameters. In the isotropic model, the minimal function values (eq 3 or 4) and the extracted τ_e values show relatively higher sensitivity to changes of the overall correlation times. The extracted τ_e values from the isotropic model do not show strong correlations with the secondary structure, similar to the patterns observed in CheA$_{1-134}$ (Zhou et al., 1995). Overall, different fitting procedures do not appear to affect the best dynamics parameters extracted (τ_m, τ_1, τ_2, and S^2) and our interpretation of the dynamics data.

While an isotropic model certainly has its drawbacks if used for cases where motional anisotropy is significant, its simple form still makes it an attractive model in many cases, especially if a proper fitting procedure and interpretation of the derived parameters are made. In our case, the distributions of the effective overall correlation times derived for each residue from the isotropic model reveal patterns of motional anisotropy for the two domains. These results are qualitively consistent with the results from the anisotropic model. The derived overall correlation times for each residue from the isotropic model can be considered as "effective correlation times" in the sense that they are weighted averages of the two correlation times derived from the anisotropic model. The weighting factor (or mixing parameter A) reflects the differences in the directions of the amide bond vectors relative to the axes of anisotropic motions if the uneven distribution in T_1/T_2 ratios is caused primarily by motional anisotropy.

Comparison of data from CheA$_{1-134}$ and CheA$_{1-233}$ has provided structural information for the phosphotransfer domain. CheA$_{1-134}$ has been shown to consist of five helices which form a compact helix bundle, with helices A to D arranged in a right-handed manner and helix E packed against helices C and D (Zhou et al., 1995). The orientation of helix E has not been well defined because of lack of long-range NOE restraints beyond Phe116. Comparison of the amide proton and nitrogen chemical shifts of CheA$_{1-134}$ and CheA$_{1-233}$ indicates that helix E is involved in stronger interaction with helix D than helix C. The residues in helix D with significant chemical shift changes, residues 90, 96, 97, and 100, are on the surface facing helix E (Figure 7). The changes in helix E, however, spread over its surface. No chemical shift changes are observed for helices A−C, suggesting they do not contact closely with helix E. The pattern of these chemical shift changes suggests possible changes in the packing of helix E with helix D.

Evidence suggests that helix E of the phosphotransfer domain does not play a significant structural role and is not required for the phosphotransfer reaction (Morrison & Parkinson, 1994; Hess et al., 1988b; Zhou et al., 1995). One possible explanation is that helix E is part of the domain linker. If so, its dynamics properties could be interesting. However, the T_1 and T_2 values and the derived dynamics parameters of helix E do not show significant differences from those of other helices both in CheA$_{1-134}$ and in

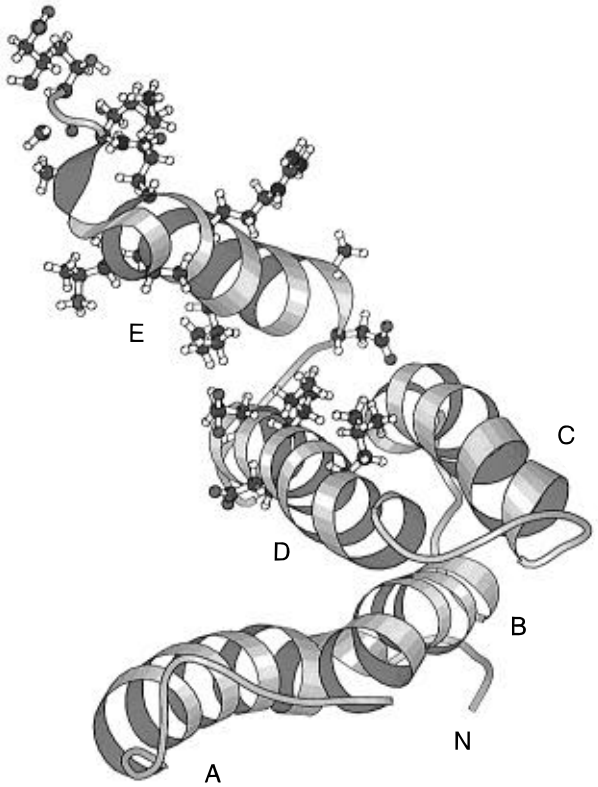

FIGURE 7: Ribbon diagram of the structure of $CheA_{1-134}$ showing the positions of those residues with relatively large amide chemical shift differences with $CheA_{1-233}$.

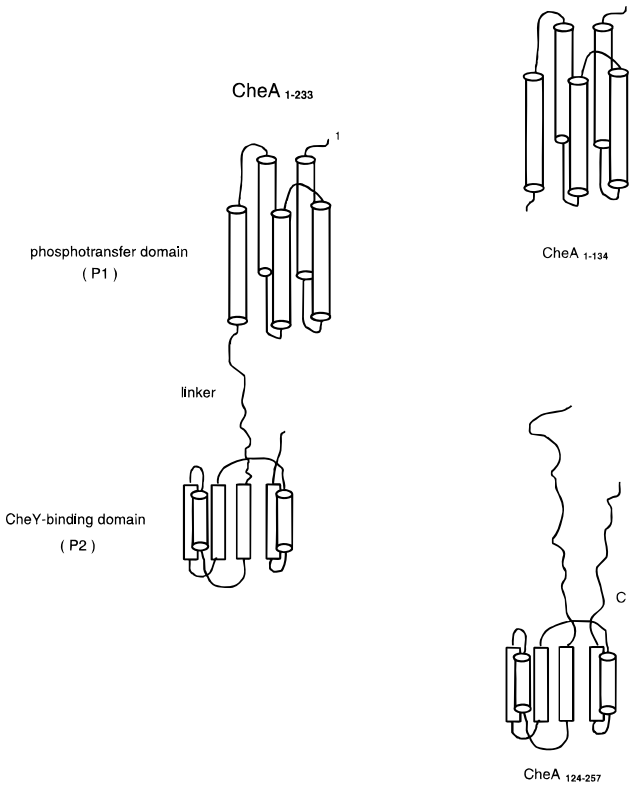

FIGURE 8: Schematic representation of the global fold of $CheA_{1-233}$ determined from studies of isolated and connected domain fragments. Also shown are the cartoons of $CheA_{1-134}$ (Zhou et al., 1995) and $CheA_{124-257}$ (McEvoy et al., 1995) from previous studies. The α-helices are shown by cylinders and the β-strands are shown by rectangles.

$CheA_{1-233}$, indicating (1) helix E is fairly rigid and is unlikely able to make large amplitude movement relative to the other four helices, and (2) helix E tumbles with the rigid frame of the phosphotransfer domain. At least dynamically, helix E belongs to the phosphotransfer domain.

Figure 8 shows a schematic representation of the structure of $CheA_{1-233}$. Also shown are the global folds of $CheA_{1-134}$ (Zhou et al., 1995) and $CheA_{124-257}$ (McEvoy et al., 1995). The possible contact between the two domains of $CheA_{1-233}$ and the properties of the linker region are the major concerns of this work. The significantly different T_1 and T_2 values, theoretically derived rotational correlation times, and properties of motional anisotropy for the P1 and P2 domains in $CheA_{1-233}$ indicate that the two domains tumble independently and appear to rule out any stable interdomain interaction. The chemical shift changes in helices D and E upon addition of the linker region and the CheY-binding domain to the C-terminus of $CheA_{1-134}$ is most likely caused by the deletion of the negatively charged carboxyl terminus and the addition of the linker region. This likely results in a slight change in the packing of helix E with helices D and C. These changes possibly involve interactions between several charged residues near the C-terminus of $CheA_{1-134}$ and those on the surfaces of helices D and C. The high flexibility of the linker region is not only reflected in the dynamic independence of the two domains but also shown by its own dynamics parameters and the chemical shift values. The residues in this region exhibit long T_2 values, low order parameters, and short τ_m values. These residues also exhibit few and weak NOEs in the 3D ^{15}N-edited NOESY and show negative $^{15}N\{^1H\}$ NOEs. Their amide proton and $C^{\alpha}H$ proton chemical shifts are also confined within the narrow ranges of random coiled values.

Comparison of the dynamics parameters of $CheA_{1-134}$ and $CheA_{1-233}$ suggests that the motional properties of one domain can be significantly affected by the flexible linker and/or the other domain even in the absence of stable interdomain contact. Except for a few residues near the N- and C-termini, $CheA_{1-134}$ is formed in a well-defined structure (Zhou et al., 1995). In $CheA_{1-233}$, $\langle T_1 \rangle$ is increased by 200 ms while $\langle T_2 \rangle$ is decreased by 30 ms relative to those of the isolated $CheA_{1-134}$, resulting in an increase of the calculated rotational correlation time $\langle \tau_m \rangle$ by ~3.5 ns. The phosphotransfer domain is approximately twice as large as the structured region of $CheA_{124-257}$, which consists of residues 159−227. Unlike the phosphotransfer domain, the experimental and derived dynamics parameters of the CheY-binding domain in $CheA_{1-233}$ are close to those in $CheA_{124-257}$ (M. M. McEvoy, D. R. Muhandiram, L. E. Kay, and F. W. Dahlquist, manuscript submitted). The properties of motional anisotropy of the two domains do not appear to be significantly changed in $CheA_{1-233}$.

The changes of molecular reorientation properties for the phosphotransfer domain in $CheA_{1-233}$ and the observed motional anisotropy of the CheY-binding domain result from direct restrictions by the flexible linker or terminal regions. The flexible linker may affect the molecular rotational correlation of the two domains in the following manner: (1) When either domain rotates, the linker is able to wrap around it and couple or restrict the motions of the two domains; (2) with an extended flexible region attached to either end of the protein, a specific rotation axis is favored so that the molecule encounters the smallest possible restriction imposed by the terminal tails. This anisotropic effect may be

significant depending on the structure of individual domains and properties of the linker.

The relaxation of two dipolar-coupled spins under anisotropic motions has been described by Woessner (1960) and Huntress (1968). For an axially symmetric molecule, the spectral density for an NH spin pair depends on the rotational diffusion coefficients $D_{||}$ and $D_{\perp}$ of the molecule and the angle (α) between the N−H bond vector and the symmetry axis and can be expressed as (Woessner, 1960):

$$J(\omega) = A_1\tau_1/[1 + (\omega\tau_1)^2] + A_2\tau_2/[1 + (\omega\tau_2)^2] + A_3\tau_3/[1 + (\omega\tau_3)^2] \quad (5)$$

with

$$A_1 = 0.75 \sin^4 \alpha \qquad \tau_1 = (4D_{||} + 2D_{\perp})^{-1}$$

$$A_2 = 3 \sin^2 \alpha \cos^2 \alpha \qquad \tau_2 = (D_{||} + 5D_{\perp})^{-1}$$

$$A_3 = (1.5 \cos^2 \alpha - 0.5)^2 \qquad \tau_3 = (6D_{\perp})^{-1}$$

An additional term should be added to eq 3 in a similar manner as in eq 1 if internal motion cannot be ignored (Barbato et al., 1992). When $\alpha = 0$, we have $A_1 = A_2 = 0$, and only the rotation perpendicular to the N−H bond vector (the third term in eq 3) contributes to relaxation. In general, rotations about the N−H bond vector do not induce time-dependent changes in the dipolar coupling Hamiltonian and therefore do not directly cause relaxation. Consequently, when a simplified form of the spectral density function (eq 1) derived under the assumption of isotropic motions is used for a nonspherical molecule in the fitting of τ_m and S^2, smaller than average τ_m of an amide ^{15}N is extracted when the preferred molecular rotation axis is perpendicular to the N−H bond vector. Larger than average τ_m is expected when the motions are parallel to the N−H bond vector. When an average rotational correlation time is used in the calculation of S^2 and τ_e values, small errors result from the differences between $\langle\tau_m\rangle$ and individual values because of the anisotropic effect (Barbato et al., 1992).

The motional anisotropy of the CheY-binding domain in $CheA_{1-233}$ is significant as indicated by the larger apparent correlation times of the two helices, especially the C-terminal helix, than those of the β sheet region. The two helices run nearly parallel to the β strands (McEvoy et al., 1995), and the N−H bond vectors of the residues in the helical region and the sheet region are nearly perpendicular (Figure 7). The rotational correlation time about a certain axis is roughly inverse to the moment of inertia about that axis. Including only the structured regions of the protein, the moments of inertia about the axes in the plane of the sheet and parallel or perpendicular to the helix axes were estimated to be roughly the same. Without considering the effect of the two random coiled terminal regions, the observed apparent motional anisotropy of the CheY-binding domain cannot be easily explained.

The rotational restrictions imposed by the flexible terminal region or domain linker are due to both the rigidity and the flexibility of the extended polypeptide chain. The former may directly cause preference of a particular rotation axis. The latter enables the chain to wrap around the adjacent rotating domain and inhibits its motion. For the CheY-binding domain in $CheA_{1-233}$ these effects cause fast rotation about the major axis parallel to the N−H bond vectors of the helical regions and slow rotation about the axis parallel to the N−H bond vectors of the sheet region, resulting in longer τ_m in the helical regions. $CheA_{124-257}$ also contains extended terminal regions, resulting in small changes in the dynamics parameters of the CheY-binding domain (M. M. McEvoy, D. R. Muhandiram, L. E. Kay, and F. W. Dahlquist, manuscript submitted).

The much larger difference of the correlation times of the phosphotransfer domain in $CheA_{1-233}$ and $CheA_{1-134}$ can also be explained by the restrictions imposed by the linker. The isolated phosphotransfer domain, $CheA_{1-134}$, shows little motional anisotropy, with $\tau_1 = 9.0 \pm 0.2$ ns and $\tau_2 = 7.0 \pm 0.2$ ns calculated using the anisotropic model, in consistency with its general fold. In $CheA_{1-233}$, the linker forces the phosphotransfer domain to rotate slowly about the direction roughly perpendicular to the long helix axis (or equivalently along the N−H bond vectors), resulting in a significant increase of the apparent rotational correlation times for most residues in this domain. The possible changes in motional anisotropy cannot be clearly identified. This is likely due to (1) the uncertainties and fluctuations in the extracted dynamics parameters which result from the lower peak intensities for the P1 domain and (2) the similar orientations for most amide bond vectors in this region which may cause apparent motional isotropy.

Recently, inverse detected two-dimensional NMR spectroscopy has been applied to study the backbone ^{15}N relaxation properties of other multidomain proteins, including calmodulin (Barbato et al., 1992) and urokinase-type plasminogen activator (u-PA) (Hansen et al., 1994), each containing two domains joined by a linker. In the studies of calmodulin the central helix joining the N- and C-terminal domains was shown to be highly flexible near the middle, resulting in effectively independent isotropic motions of the two domains. In the case of u-PA, differences in motional anisotropy of the two domains were observed and explained by their motional independence. In the latter case the dynamics properties of the linker region is not clear. In both studies no stable interdomain contacts were detected. These studies have provided dynamic pictures of interdomain interactions in multidomain proteins. However, effects of the linker regions on molecular rotational correlations have not been addressed. To do so, direct comparison of the dynamics parameters of the multidomain protein and its isolated domain fragments are required. In one study (Nowak et al., 1993) direct comparison of the dynamics parameters was made for a three-domain u-PA protein based on line width analysis and has not provided as detailed and accurate information as from backbone dynamics studies. It is worth noting that the flexible linker regions in calmodulin and u-PA are only 4−6 residues long and the motions of the two domains are essentially hinged motions.

In our studies we have shown that long domain linkers or extended terminal flexible regions have direct and significant effects on the molecular rotational properties of the constituent domains. In our case rotational restrictions from direct interdomain coupling are not as important as those imposed directly by the linker. An extra anisotropic effect can be induced by the linker and coupled to the intrinsic molecular isotropic or anisotropic motions, resulting in more isotropic or anisotropic motions. It is conceivable that the motional

coupling among the linker and domains also depends on their relative sizes or length. There possibly is a critical length for each domain linker longer than which only linker effects on the motional properties of the domains are important and shorter than which direct domain−domain coupling is dominant. The terminal random-coiled regions of the CheY-binding domain in $CheA_{1-233}$ and $CheA_{124-257}$ might be much longer than this critical length so that remote changes at these terminal regions do not further affect the dynamics of this domain. This is consistent with the usual estimate of presence lengths of three or four residues for random peptides lacking proline (Cantor & Schimmel, 1980).

Other extended linker regions of the CheA molecule may have similar structure and dynamics properties with the one joining P1 and P2. These linkers are possibly made to keep various components of CheA in proximity so that during the signal transduction a quick and proper response to extracellular signal is induced. If so, the linker regions play very passive functional roles. In vivo signal transduction involves a number of proteins functioning within or through protein complexes. Each of the constituent domains of CheA has to properly respond to input signals and generate specific output signals. Signaling and reponding events must be integrated into a delicate and possibly unique information flow. One obvious advantage with the use of flexible linkers in CheA is the dramatic reduction of wasteful molecular diffusion and randomness in the spatial organization of various functional components without loss of flexibility. Design of these domain linkers could be delicate. Arbitrary length or sequence may structurally or dynamically block the interaction pathway and result in inefficient functional activities.

The effective structural and dynamic independence of the constituent domains of CheA suggests that these domains have independent functions. In addition, the activity of each domain could then be controlled nearly independently. This may allow a complex signal transduction system to respond properly to a wide range of situations. The flexible linkers between domains also make possible different sequential organizations of so-called "communication modules" of bacterial signaling systems (Parkinson & Kofoid, 1992). The possible functional roles of differing sequential organization of domains remain unclear. It is possible that the only role of the linkers is to sequester all of the functional domains to the same localized volume. In this circumstance, diffusion of ligands between domains could be enhanced while each domain could retain its functional independence from the others.

The CheA autokinase plays a pivotal rule in bacterial chemotaxis as part of a ternary complex with transmembrane receptors and a coupling protein CheW. The autophosphorylation activity is regulated by binding events on the extracytoplasmic surface of the receptors and by methylation at four glutamate residues on the cytoplasmic side of the receptors. The combination of the ligand binding and multiple methylation produces a number of activity states covering about two orders of magnitude in activity. This presents an intriguing problem: How can a discrete active site be characterized by such a large number of graded activities? The input and output domains of the receptors are joined by a long transmembrane helix bundle (Milburn et al., 1991). Conformational changes are transmitted and possibly amplified by the transmembrane segment of the dimeric receptors to their cytoplasmic domains (Stock et al., 1991; Parkinson & Kofoid, 1992). The intra- or intersubunit movements of the dimeric receptors may force subsequent rotational movement of the subunits of the CheA dimer relative to each other (Parkinson & Kofoid, 1992) through the receptor−CheW−CheA complex. This movement may subsequently decrease or increase the distance between the autophosphorylation site of one subunit and the catalytic site of the other. These changes may effectively regulate the CheA autokinase activity in a positive or negative manner.

Our observation of independent motion of the phosphotransfer domain suggests a molecular model to explain various kinase activity states. In this model we propose that the diffusional access of the phosphotransfer domain to the kinase is regulated by events in the receptors. Thus, autophosphorylation activity could be lowered by increasing the mean distance or providing steric interference reducing access of the phosphotransfer domain to the kinase domain. Because the linker is relatively short, the regulated access of a tethered but noninteractory domain could be much more finely tuned than if the phosphotransfer domain was independent. This is especially true if the kinase domain acts on the phosphotransfer domain of the other subunit in the dimer as has been observed (Wolfe & Stewart, 1993).

SUPPORTING INFORMATION AVAILABLE

Two tables listing the chemical shifts of the amide groups and side chain protons of 210 residues and the values and errors of the experimental ^{15}N T_1, T_2, and NOE values together with the calculated rotational correlation times (τ_m, τ_1, and τ_2), order parameter, S^2, and correlation time for internal motion, τ_e, for the isotropic model or the anisotropic model (11 pages). Ordering information is given on any current masthead page.

REFERENCES

Barbato, G., Ikura, M., Kay, L. E., Paster, R. W., & Bax, A. (1992) *Biochemistry 31*, 5269−5278.
Billeter, M., Neri, D., Otting, G., Qian, Y. Q., & Wüthrich, K. (1992) *J. Biomol. NMR 2*, 257−274.
Bodenhausen, G., Kogler, H., & Ernst, R. R. (1984) *J. Magn. Reson. 58*, 5485−5489.
Borkovich, K. A., & Simon, M. I. (1990) *Cell 63*, 1339−1348.
Borkovich, K. A., Kaplan, N., Hess, J. F., & Simon, M. I. (1989) *Proc. Natl. Acad. Sci. U.S.A. 86*, 1208−1212.
Borkovich, K. A., Alex, L. A., & Simon, M. I. (1992) *Proc. Natl. Acad. Sci. U.S.A. 89*, 6756−6760.
Bourret, R. B., Borkovich, K. A., & Simon, M. I. (1991) *Annu. Rev. Biochem. 60*, 401−441.
Cantor, C. R., & Schimmel, P. R. (1980) *Biophysical Chemistry*, W. H. Freeman and Co., New York.
Cavanagh, J., Chazin, W. J., & Rance, M. (1989) *J. Magn. Reson. 87*, 110−131.
Clore, G. M., Driscoll, P. C., Wingfield, P. T., & Gronenborn, A. M. (1990) *Biochemistry 29*, 7387−7401.
Englander, S. W., & Wand, A. J. (1987) *Biochemistry 26*, 5953−5958.
Garrett, D. G., Powers, R., March, C. J., Frieden, E. A., Clore, G. M., & Gronenborn, A. M. (1992) *Biochemistry 31*, 4547−4553.
Gegner, J. A., Graham, D. R., Roth, A. F., & Dahlquist, F. W. (1992) *Cell 70*, 975−982.
Hansen, A. P., Petros, A. M., Meadows, R. P., & Fesik, S. W. (1994) *Biochemistry 33*, 15418−15424.
Hess, J. F., Oosawa, K., Kaplan, N., & Simon, M. I. (1988a) *Cell 53*, 79−87.
Hess, J. F., Bourret, R. B., & Simon, M. I. (1988b) *Nature 336*, 139−143.

Huntress, W. T. (1968) *J. Chem. Phys. 48*, 3524−3533.
Kay, L. E., & Bax, A. (1990) *J. Magn. Reson. 86*, 110−126.
Kay, L. E., Torchia, D. A., & Bax, A. (1989a) *Biochemistry 28*, 8972−8979.
Kay, L. E., Marion, D., & Bax, A. (1989b) *J. Magn. Reson. 84*, 72−84.
Karplus, M. (1995) *J. Phys. Chem. 30*, 11−15.
Kumar, A., Wüthrich, K., & Ernst, R. R. (1980) *Biochem. Biophys. Res. Commun. 95*, 1−6.
Lipari, G., & Szabo, A. (1992) *J. Am. Chem. Soc. 104*, 4546−4558.
Lupas, A., & Stock, J. (1989) *J. Biol. Chem. 264*, 17337−17342.
Macura, S., & Ernst, R. R. (1980) *Mol. Phys. 41*, 95−117.
Marion, D., Ikura, M., Tschudin, R., & Bax, A. (1989) *J. Magn. Reson. 85*, 393−399.
McEvoy, M. M., Zhou, H., Roth, A. F., Lowry, D. L., Morrison, T. B., Kay, L. E., & Dahlquist, F. W. (1995) *Biochemistry 34*, 13871−13880.
McNally, D. F., & Matsumura, P. (1991) *Proc. Natl. Acad. Sci. U.S.A. 88*, 6269−6273.
Milburn, M. V., Privé, G. G., Milligan, D. L., Scott, W. G., Yeh, J., Jancarik, J., Koshland, D. E., & Kim, S.-H. (1991) *Science 254*, 1342−1347.
Morrison, T., & Parkinson, J. S. (1994) *Proc. Natl. Acad. Sci. U.S.A. 91*, 5485−5489.
Ninfa, E. G., Stock, A., Mowbray, S., & Stock, J. (1991) *J. Biol. Chem. 266*, 9764−9770.
Nowak, U. K., Li, A., Teuten, A. J., Smith, R. A. G., & Dobson, C. M. (1993) *Biochemistry 32*, 298−309.
Parkinson, J. S., & Kofoid, E. C. (1992) *Annu. Rev. Genet. 26*, 71−112.
Presnell, S. R., & Cohen, F. E. (1989) *Proc. Natl. Acad. Sci. U.S.A. 86*, 6592−6596.
Press, W. H., Teukolsky, S. A., Vetterling, W. T., & Hannery, B. P. (1992) *Numerical Recipes*, Cambridge University Press, England.
Roman, S. J., Meyers, M., Voltz, K., & Matsumura, P. (1992) *J. Bacteriol. 174*, 6247−6255.
Sanders, D. A., Gillece-Castro, B. L., Stock, A. M., Burlingame, A. L., & Koshland, D. E., Jr. (1989) *J. Biol. Chem. 264*, 21770−21778.
Smith, R. A., & Parkinson, J. S. (1980) *Proc. Natl. Acad. Sci. U.S.A. 77*, 5370−5374.
Stewart, R. C., & Dahlquist, F. W. (1987) *Chem. Rev. 87*, 997−1025.
Stock, A. M., Wylie, D. C., Mottonen, J. M., Lupas, A. N., Ninfa, E. G., Ninfa, A. J., Schutt, C. E., & Stock, J. B. (1988) *Cold Spring Harbor Symp. Quant. Biol. 53*, 49−57.
Stock, J. B., Ninfa, A. J., & Stock, A. M. (1989) *Microbiol. Rev. 53*, 450−490.
Stock, J. B., Lukat, G. S., & Stock, A. M. (1991) *Annu. Rev. Biophys. Biophys. Chem. 20*, 109−136.
Swanson, R. V., Schuster, S. C., & Simon, M. I. (1993) *Biochemistry 32*, 7623−7629.
Tjandra, N., Kuboniwa, H., Ren, H., & Bax, A. (1995) *Eur. J. Biochem. 230*, 1014−1024.
Woessner, D. T. (1962) *J. Chem. Phys. 37*, 647−654.
Wolfe, A. J., & Stewart, R. C. (1993) *Proc. Natl. Acad. Sci. U.S.A. 90*, 1518−1522.
Wüthrich, K. (1986) *NMR of Proteins and Nucleic Acids*, Wiley, New York.
Wylie, D., Stock, A., Wong, C.-Y., & Stock, J. (1988) *Biochem. Biophys. Res. Commun. 151*, 891−896.
Zhou, H., Lowry, D. F., Swanson, R. V., Simon, M. I. & Dahlquist, F. W. (1995) *Biochemistry 34*, 13858−13870.
Zuiderweg, E. R. P. (1990) *J. Magn. Reson. 86*, 346−357.
Zuiderweg, E. R. P., & Fesik, S. W. (1989) *Biochemistry 28*, 2387−2391.
Zuiderweg, E. R. P., Hallenga, K., & Olejniczak, E. T. (1986) *J. Magn. Reson. 70*, 336−343.

BI951960E